

## **CHAPTER 3. DESIGN OF HIGH-BIREFRINGENCE AND SINGLE-POLARIZATION SINGLE-MODE FIBERS**

In general, polarization-maintaining fibers can be categorized as high-birefringence fibers, and single-polarization single-mode fibers. In this chapter, the two categories of polarization-maintaining fibers will be addressed. A number of fiber refractive-index profiles will be investigated and discussed along with their design parameters and characteristics in order to achieve high-birefringence or single-polarization single-mode fibers. The dispersion characteristics of these fibers will also be studied and optimized to obtain a zero dispersion at the operating wavelength.

### **3.1 POLARIZATION-MAINTAINING FIBERS**

#### **3.1.1 Anisotropic Fibers**

Birefringence in optical fibers can be obtained by geometrical, stress, or a combination of both effects. In a large number of cases, the stress-induced birefringence (material birefringence) is much larger than that produced by a noncircular geometry (geometric birefringence) of the core.

Here, we focus attention on anisotropy-based fiber designs and determine optimum parameters to achieve both high birefringence and zero dispersion at the operating wavelength. The presence of anisotropy in a fiber results in two different refractive-index profiles along the  $x$  and  $y$  axes. Thus, the propagation of  $x$ -polarized and  $y$ -polarized fundamental modes depend on the  $x$  and  $y$  refractive-index profiles, respectively.

The analysis presented in this investigation pertains to weakly guiding and weakly anisotropic fibers. Stress-induced anisotropy can be described in terms of a stress tensor. By orienting the coordinate system axes so that they coincide with the principal axes of the

stress tensor, the diagonal elements of the tensor,  $\sigma_x$ ,  $\sigma_y$ , and  $\sigma_z$ , are the only non-zero entries. Then, the refractive index changes can be expressed as follows [108]

$$n_x - n = (-n^3/2)(p_{11}\sigma_x + p_{12}\sigma_y + p_{12}\sigma_z) \quad (3.1a)$$

$$n_y - n = (-n^3/2)(p_{12}\sigma_x + p_{11}\sigma_y + p_{12}\sigma_z) \quad (3.1b)$$

$$n_z - n = (-n^3/2)(p_{12}\sigma_x + p_{12}\sigma_y + p_{11}\sigma_z) \quad (3.1c)$$

where  $n_x$ ,  $n_y$ , and  $n_z$  are the components of the refractive index  $n$  in the  $x$ ,  $y$ , and  $z$  directions, respectively. The coefficients  $p_{11}$  and  $p_{12}$  are the stress-optical coefficients, which are also called photoelastic constants. Assuming the stress exists only in the  $y$ - $z$  plane,  $\sigma_x = 0$ , the birefringence of the material for a plane wave traveling in the  $z$ -direction can be obtained as

$$B = n_x - n_y = (n^3/2)(p_{11} - p_{12})\sigma_y \quad (3.2)$$

For silica glass, a typical value for  $B$  is  $5 \times 10^{-4}$ . The photoelastic constants  $p_{11}$  and  $p_{12}$  for silica have been determined to be 0.12 and 0.27, respectively [108]-[109]. The principal stress distributions in the  $y$  and  $z$  directions are assumed to be equal,  $\sigma_y = \sigma_z$ . The wavelength dependence of  $n_x$  and  $n_y$  is approximated by that of  $n$  and is determined using the Sellmeier equation which is expressed as [110]

$$n(\lambda) = \left\{ 1 + \sum_{i=1}^3 \left[ \frac{A_i \lambda^2}{\lambda^2 - \lambda_i^2} \right] \right\}^{1/2} \quad (3.3)$$

where  $\lambda_i$  and  $A_i$ ;  $i = 1, 2, 3$ , are the Sellmeier coefficients whose measured values are available for a number of silica-based materials used for fiber fabrication.

Calculating  $\sigma_y$  from (3.2) with  $B = 5 \times 10^{-4}$  and  $n = n(\lambda=1.55\mu\text{m})$  used in it, the expressions for  $n_x$  and  $n_y$  are summarized as

$$n_x = n(\lambda) - 594 \times 10^{-6} (n^3(\lambda)) \quad (3.4a)$$

$$n_y = n(\lambda) - 429 \times 10^{-6} (n^3(\lambda)) \quad (3.4b)$$

### 3.2 ANALYSIS

In this analysis, the polarization-maintaining fiber is a circularly cylindrical anisotropic waveguide consisting of a central core region and several claddings. The formulation used here will be applicable to structures with one to three cladding layers. All layers are assumed to be lossless, linear, and nonmagnetic. The  $i$ th layer, with  $i = 1$  representing the core and  $i > 1$  referring to the cladding regions, is characterized by a radius  $r_i$  and refractive index  $n_i$ .  $n_i$  is the index in the absence of anisotropy due to applied stress, and is used in (3.4a) and (3.4b) to determine indices along  $x$  and  $y$  axes. The outer cladding layer is assumed to extend to infinity in the radial direction because the field of guided modes decay exponentially in the radial direction in this cladding. A cylindrical coordinate system  $(r, \phi, z)$  is chosen and propagation of electromagnetic fields along the positive  $z$ -direction is considered. The time and  $z$  dependence of fields is assumed to be as  $e^{j(\omega t - \beta z)}$ , where  $\beta$  is the axial propagation constant, and is  $\beta_x$  for  $x$ -polarized mode and  $\beta_y$  for  $y$ -polarized mode. Various refractive index profiles used in this investigation are shown in Figure 3.1. For weakly guiding anisotropic fibers, the fields for  $x$ - and  $y$ -polarized modes are the solutions of the scalar-wave equation with  $x$ - and  $y$ -polarized indices used in it [106].

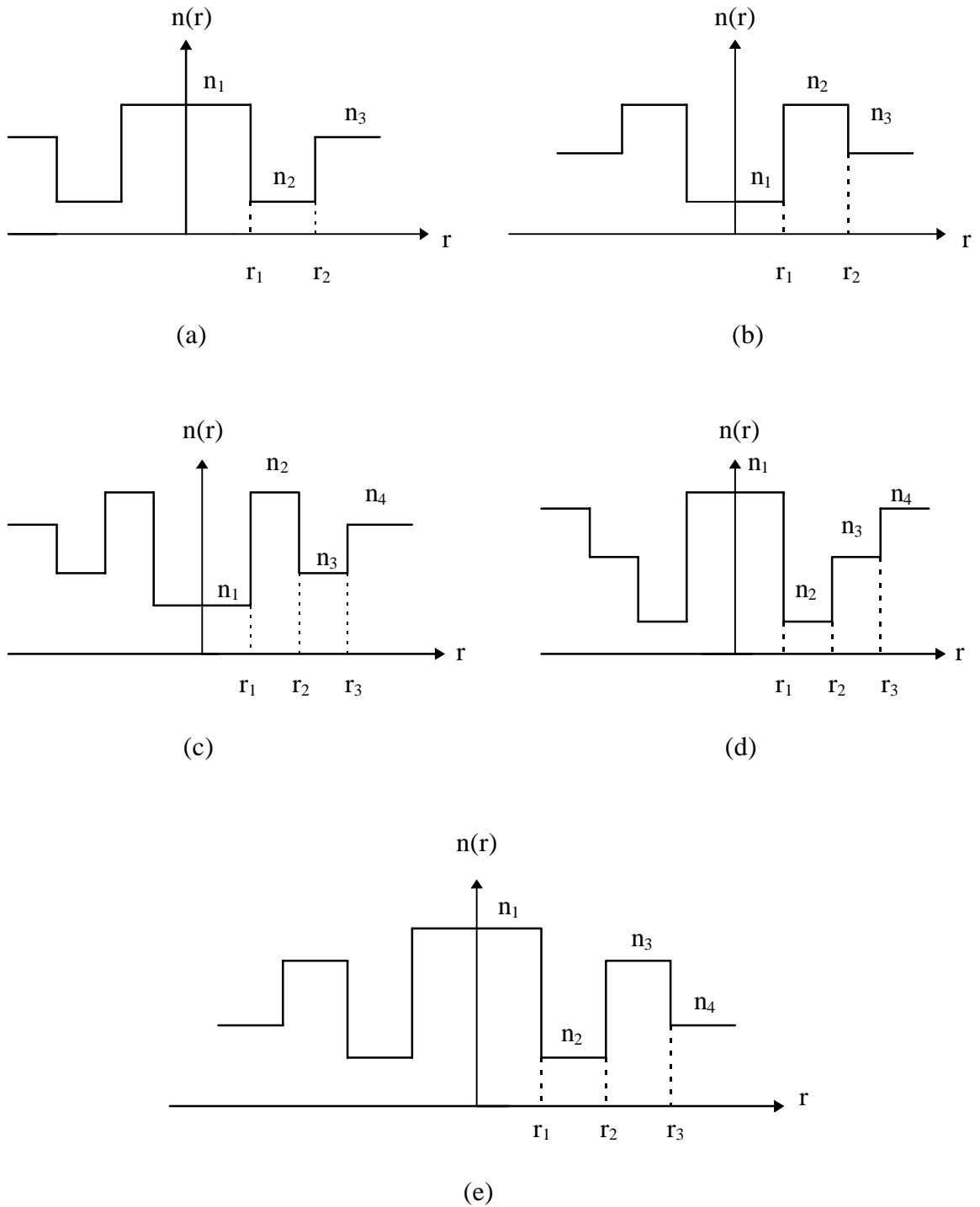


**Figure 3.1** Refractive-index profiles used for the design of high-birefringence and single-polarization single-mode fibers.

### 3.2.1 Propagation Constant and Birefringence

For triple-clad fibers, there are three boundaries. Using the scalar-wave analysis, boundary conditions reduce to the continuity of the scalar field component  $\psi(r,\phi)$  and its derivative  $\partial\psi(r,\phi)/\partial r$ . By imposing the boundary conditions, the characteristic equation can be obtained. In general, the characteristic equation is a function of wavelength  $\lambda$ , propagation constant  $\beta$ , azimuthal number  $v$ , layers radii  $r_i$  and their refractive indices  $n_i$ , where  $i = 1, 2, 3, \dots, N$  for  $N$  layer structures. It may be expressed as

$$f(\lambda, \beta, v, r_i, \text{ and } n_i, i = 1, 2, 3, \dots, N) = 0 \quad (3.5)$$

The propagation constant  $\beta$  is found as a function of wavelength  $\lambda$  when all fiber parameters and  $v$  are specified. The method used to solve for the propagation constant  $\beta$  is a numerical root search technique. In solving (3.5) for  $\beta$ , the layers' material compositions are chosen and the variations of their refractive indices with wavelength are accounted for by the Sellmeier equation. A normalized propagation constant is defined as

$$b = (\bar{\beta}^2 - n_N^2) / (n_{\max}^2 - n_N^2) \quad (3.6)$$

where  $n_N$  is the refractive index of the outer cladding layer, and  $n_{\max}$  is the highest refractive index in the examined profile. Based on this definition and noting that for guided modes  $n_N < \bar{\beta} < n_{\max}$ , the value of  $b$  will always vary between 0 and 1, irrespective of the refractive index values or profile shape.

An important property of polarization-maintaining fibers is birefringence which essentially is a measure of isolation between the  $x$ - and  $y$ -polarized modes. It is defined as

$$B = \bar{\beta}_y - \bar{\beta}_x \quad (3.7)$$

The larger the value of  $B$ , the more unlikely the coupling of the two polarizations of a mode. Birefringence is one of the principal design parameter, and polarization-maintaining fibers should be designed such that  $B$  is maximized.

### 3.2.2 Dispersion

The chromatic dispersion in a single-mode fiber is due to waveguiding property of the fiber structure as well as the dispersive property of the fiber materials. Material dispersion is caused by the materials' refractive index variations with wavelength. Waveguide dispersion is caused by the existence of boundaries in the fiber structure. Aside from material and waveguide dispersion, there also exists polarization-mode dispersion in single-mode fibers which is mainly caused by slight deviation of the core being perfectly circular. This slight deviation, usually in the form of ellipticity, causes a small difference between the propagation constants of the two-orthogonally-polarized fundamental modes of a circular isotropic fiber, i.e. x- and y-polarized modes, which results in pulse spreading over the fiber length. Polarization-mode dispersion and pertinent fiber designs to avoid it are thoroughly discussed in Chapter 4.

Considering that only the fundamental  $LP_{01}$  mode propagates in the fiber, the chromatic dispersion expression can be written as

$$D = - (\lambda/2\pi c) (2 d\beta/d\lambda + \lambda d^2\beta/d\lambda^2) \quad (3.8a)$$

$$= - (\lambda/c)(d^2 \bar{\beta}/d\lambda^2) \quad (3.8b)$$

where  $c$  is the velocity of light in free space and  $\bar{\beta} = \lambda\beta/2\pi$ .

In order to evaluate the chromatic dispersion, the approximation that the waveguide and material dispersion are additive may be satisfactory for ordinary single-mode fibers, but this approximation may not be adequate when designing ultra-low dispersion fibers [111].

Therefore, in this investigation, material and waveguide dispersion are accounted for simultaneously. That is, the propagation constant  $\beta$  is calculated by numerically solving the characteristic equation (3.5), in which the dependence of refractive indices on wavelength is accounted for by using the Sellmeier equation (3.3). Having found the propagation constant  $\beta$ , the terms for  $d\beta/d\lambda$  and  $d^2\beta/d\lambda^2$  are determined by numerical differentiation. The dispersion as a function of wavelength is then obtained from (3.8b). In high-birefringence fibers,  $D$  is calculated for the x- or y-polarized  $LP_{01}$  mode by using  $\bar{\beta}_x$  or  $\bar{\beta}_y$  in (3.8b), respectively.

### **3.3 FIBER DESIGNS**

#### **3.3.1 High-Birefringence Fibers**

The goal of the design is to simultaneously obtain zero dispersion and high birefringence at the operating wavelength. The design procedure involves three steps. First, an isotropic profile resulting in zero total dispersion at the wavelength of operation is considered. In the second step, materials whose refractive indices, after being subjected to a given stress, match or are close to the indices of the isotropic profile are selected. The design obtained, after these two steps are carried out, does not generally maintain zero dispersion at the wavelength of operation. The third step is to adjust the radii and the material composition of various layers to meet the dispersion requirement. The material compositions used for the designs presented in this work are listed in Table 3.1. In this section, five high-birefringence fiber designs labeled as F1 to F5 are presented.

##### **3.3.1.1 Dispersion-Flattened Fibers**

The profiles shown in Figure 3.1a and 3.1d, corresponding to W-type and triple-clad fibers, respectively, provide dispersion-flattened characteristics. The material compositions and radii of these fibers, labeled as F1 and F2, respectively, are summarized in Table 3.2. Figures 3.2 and 3.3 show variations of the normalized propagation constant  $b$  versus wavelength for the y- and x-polarized fundamental  $LP_{01}$  modes, respectively.

**Table 3.1 Compositions of Materials Used in The Design of Polarization-Maintaining Fibers.**

<b>Material Designation</b>	<b>Material Compositions</b>
M1	Pure Silica
M2	13.5 m/o GeO <sub>2</sub> , 86.5 m/o SiO <sub>2</sub>
M3	7.0 m/o GeO <sub>2</sub> , 93.0 m/o SiO <sub>2</sub>
M4	4.1 m/o GeO <sub>2</sub> , 95.9 m/o SiO <sub>2</sub>
M5	9.1 m/o GeO <sub>2</sub> , 7.7 m/o B <sub>2</sub> O <sub>3</sub> , 83.2 m/o SiO <sub>2</sub>
M6	0.1 m/o GeO <sub>2</sub> , 5.4 m/o B <sub>2</sub> O <sub>3</sub> , 94.5 m/o SiO <sub>2</sub>
M7	3.1 m/o GeO <sub>2</sub> , 96.9 m/o SiO <sub>2</sub>
M8	3.5 m/o GeO <sub>2</sub> , 96.5 m/o SiO <sub>2</sub>
M9	5.8 m/o GeO <sub>2</sub> , 94.2 m/o SiO <sub>2</sub>
M10	7.9 m/o GeO <sub>2</sub> , 92.1 m/o SiO <sub>2</sub>
M11	3.5 m/o B <sub>2</sub> O <sub>2</sub> , 96.5 m/o SiO <sub>2</sub>
M12	3.3 m/o GeO <sub>2</sub> , 9.2 m/o B <sub>2</sub> O <sub>3</sub> , 87.5 m/o SiO <sub>2</sub>
M13	2.2 m/o GeO <sub>2</sub> , 3.3 m/o B <sub>2</sub> O <sub>3</sub> , 94.5 m/o SiO <sub>2</sub>
M14	9.1 m/o P <sub>2</sub> O <sub>5</sub> , 90.9 m/o SiO <sub>2</sub>



**Table 3.2 Materials and Radii for Polarization-Maintaining Dispersion-Flattened Fibers.**

<b>Fiber</b>	<b>Index Profile</b>	<b>Core</b>	<b>Clad1</b>	<b>Clad2</b>	<b>Clad3</b>
<b>F1</b>	<b>Fig. 3.1a</b>	M14 3 $\mu\text{m}$	M6 5.65 $\mu\text{m}$	M4 $\infty$	—
<b>F2</b>	<b>Fig. 3.1d</b>	M14 3 $\mu\text{m}$	M12 3.6 $\mu\text{m}$	M13 5.9 $\mu\text{m}$	M4 $\infty$

These figures, in addition to fibers F1 and F2, also show the propagation characteristics for three other fibers, labeled as F3, F4, and F5, which will be addressed later. The cutoff wavelength for the x-polarized  $\text{LP}_{01}$  mode of both fibers is about the same and equal to 1.66  $\mu\text{m}$ . The cutoff wavelength for the y-polarization of these two profiles is also about the same and equal to 1.77  $\mu\text{m}$ . Table 3.3 indicates that the y-polarization of the next higher mode has a cutoff below 0.95  $\mu\text{m}$ , which is higher than the x-polarization cutoff for the  $\text{LP}_{11}$  mode. Hence, the x- and y-polarized  $\text{LP}_{01}$  modes are the only modes that exist in the wavelength range  $0.95 \mu\text{m} < \lambda < 1.77 \mu\text{m}$ . All other modes have cutoffs at lower wavelengths than that of the y-polarization  $\text{LP}_{11}$  mode.

Variations of birefringence versus wavelength for the two fibers are illustrated in Figure 3.4. The two profiles exhibit the same birefringence values for wavelengths below 1.5  $\mu\text{m}$ . For  $\lambda > 1.55 \mu\text{m}$ , the birefringence of the W-fiber profile is slightly less than that of the triple-clad fiber. The birefringence values at wavelengths 1.33  $\mu\text{m}$  and 1.55  $\mu\text{m}$  are  $5.11 \times 10^{-4}$  and  $4.87 \times 10^{-4}$ , respectively. In general, the birefringence, as Figure 3.4 indicates, decreases with wavelength and the decrease becomes more rapid as cutoff wavelength is approached. The decrease in birefringence for these profiles over the wavelength range  $1 \mu\text{m} < \lambda < 1.66 \mu\text{m}$  is about  $1 \times 10^{-4}$ .

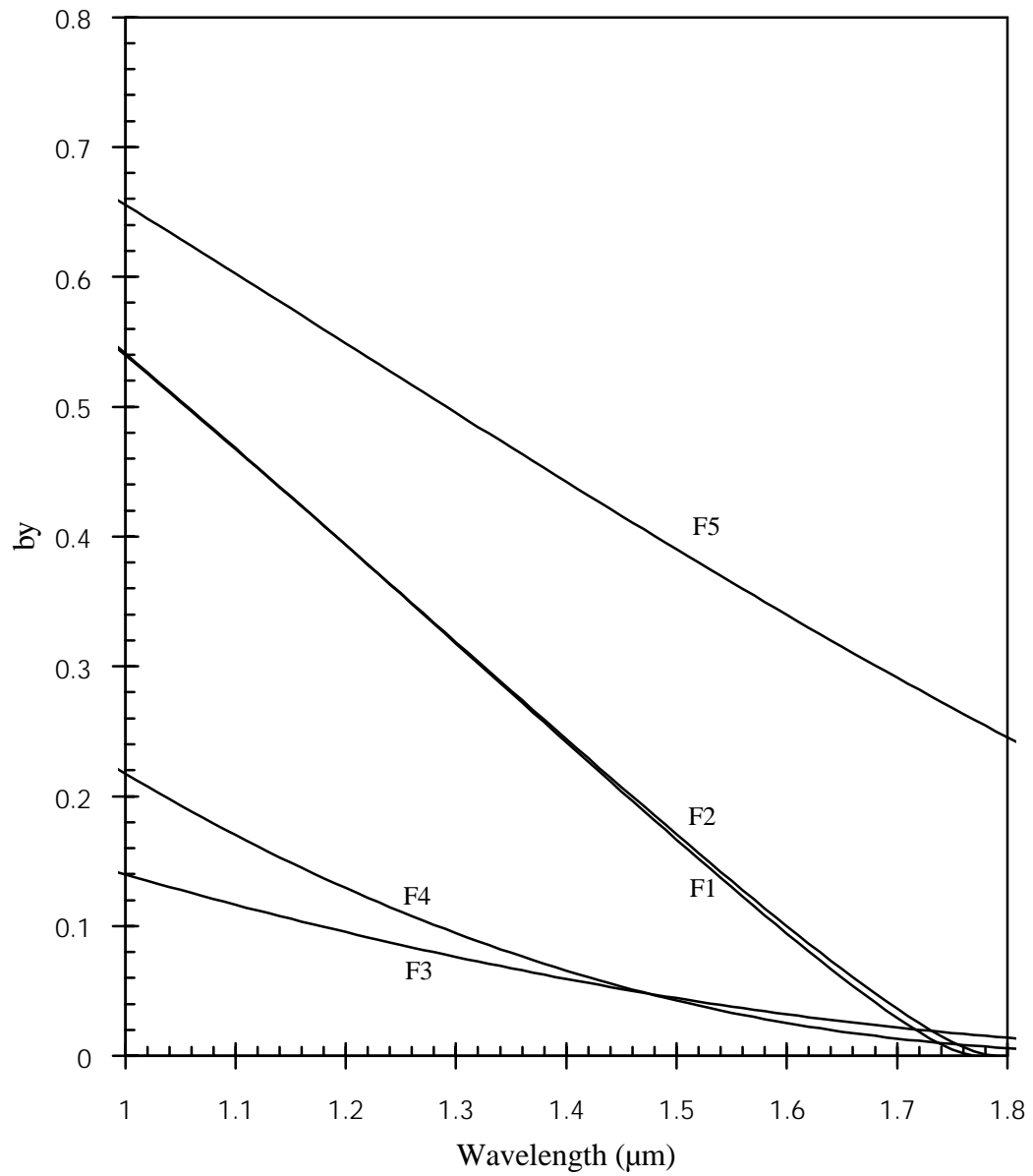


**Figure 3.2 Normalized propagation constant versus wavelength for the y-polarization of fundamental LP<sub>01</sub> mode for fibers F1 to F5.**

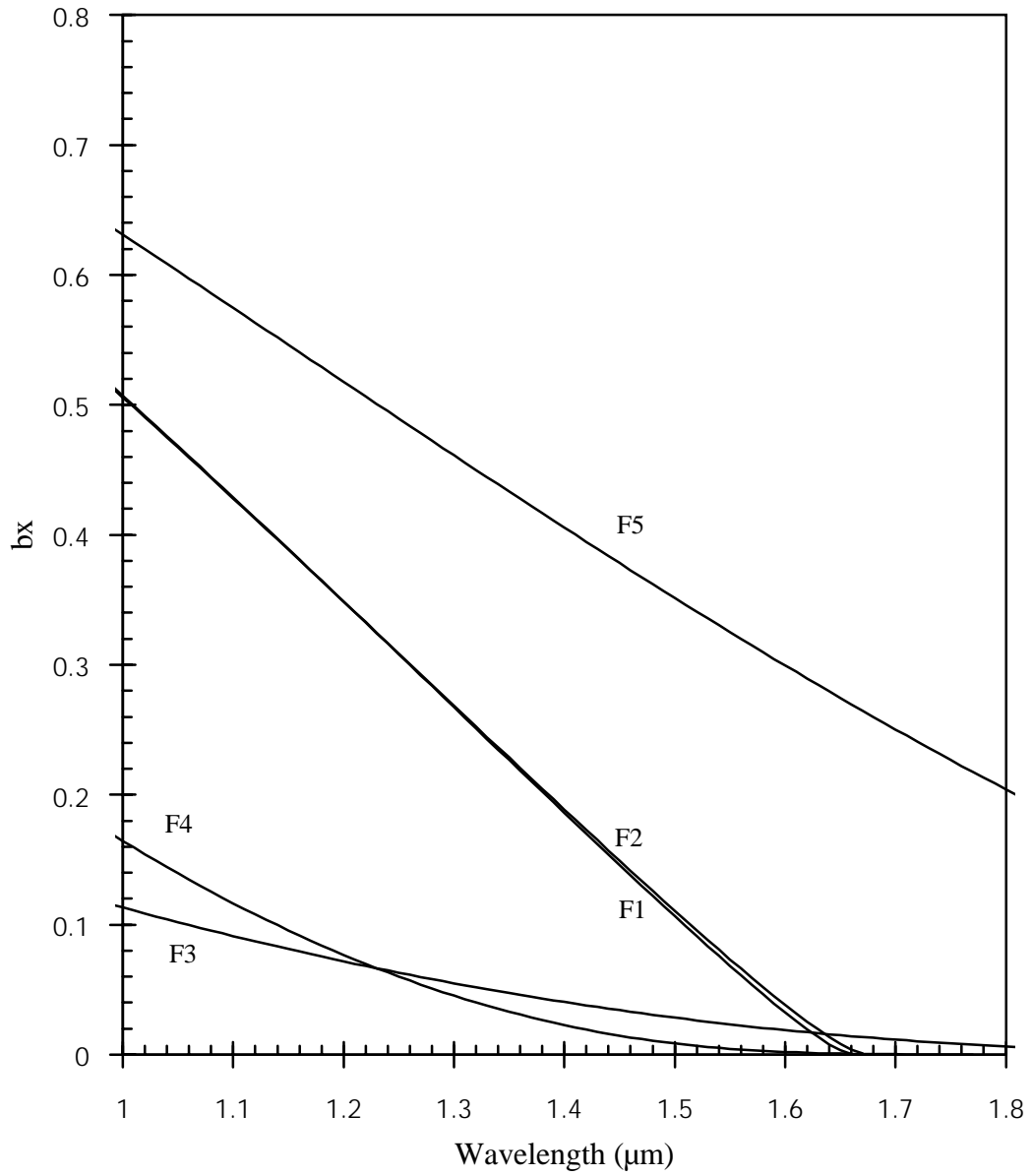


**Figure 3.3 Normalized propagation constant versus wavelength for the x-polarization of fundamental  $LP_{01}$  mode for fibers F1 to F5.**

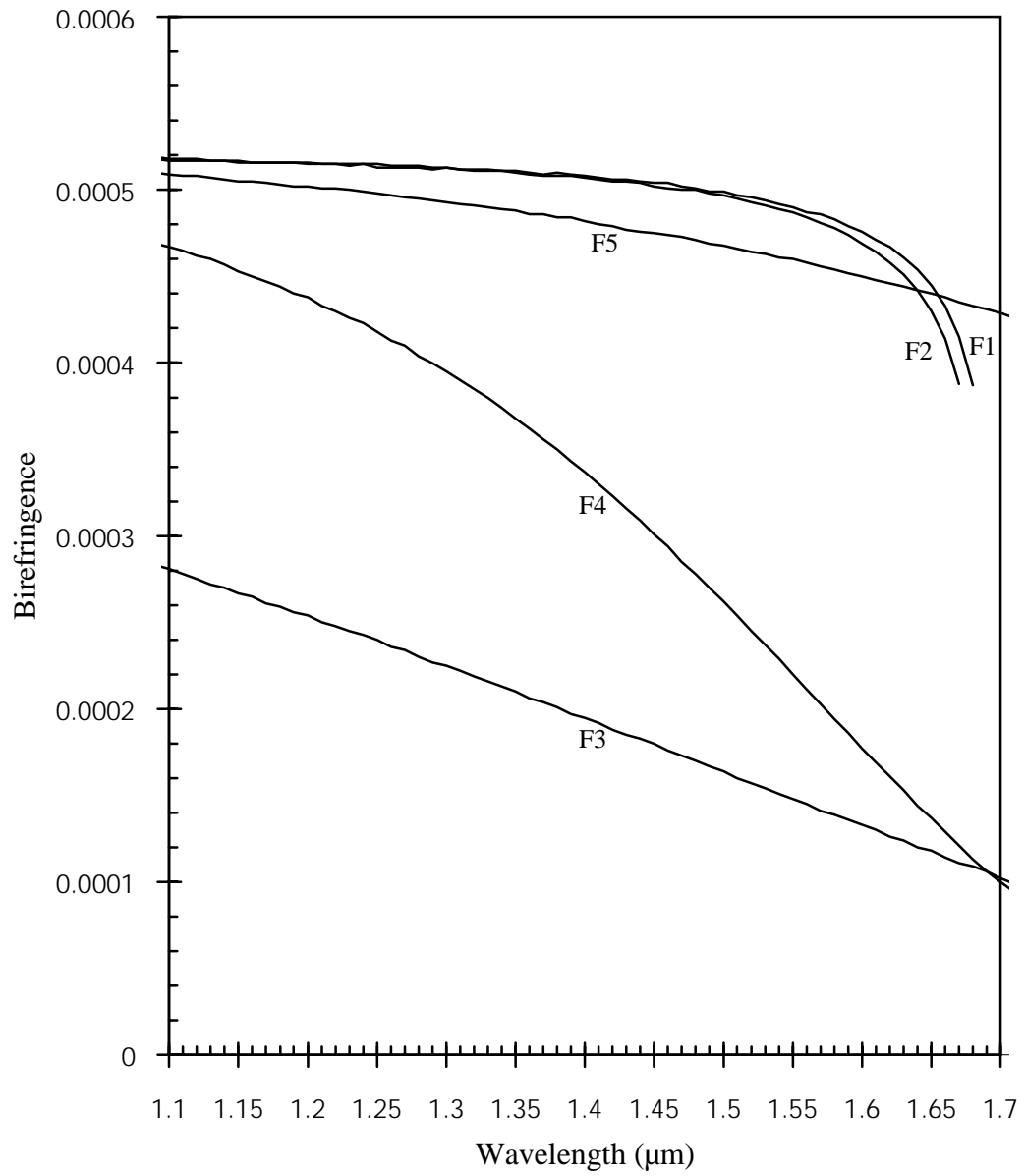


**Figure 3.4 Birefringence versus wavelength for fibers F1 to F5.**

**Table 3.3 Cutoff Wavelength of The LP<sub>11</sub> Mode For the Designed Fibers.**

<b>Fiber</b>	<b>Cutoff Wavelength of LP<sub>11</sub> Mode</b>
F1	0.92 $\mu\text{m}$
F2	0.92 $\mu\text{m}$
F3	1.12 $\mu\text{m}$
F4	0.95 $\mu\text{m}$
F5	1.18 $\mu\text{m}$
F6	1.0 $\mu\text{m}$
F7	0.97 $\mu\text{m}$
F8	0.84 $\mu\text{m}$
F9	1.27 $\mu\text{m}$

The dispersion variation of the y-polarized fundamental mode versus wavelength shown in Figure 3.5 indicates that the dispersion for both fibers F1 and F2 at  $\lambda = 1.55 \mu\text{m}$  is equal to or close to zero (-0.1 ps/nm.km) while the dispersion at  $\lambda = 1.33 \mu\text{m}$  is 0.65 ps/nm.km. Actually, the dispersion goes to zero at 1.32  $\mu\text{m}$  and 1.34  $\mu\text{m}$  for fibers F1 and F2, respectively. The F1 fiber exhibits a dispersion of less than 4 ps/nm.km over the wavelength range  $1.32 \mu\text{m} < \lambda < 1.55 \mu\text{m}$ , while fiber F2 gives lower dispersion value of less than 3 ps/nm.km over the wavelength range  $1.34 \mu\text{m} < \lambda < 1.55 \mu\text{m}$ . In general, fibers F1 and F2 have very much similar general behavior and characteristics in terms of cutoff wavelength, propagation constant, and birefringence variations versus wavelength. However, the dispersion curves for the two fibers are a little different.

### **3.3.1.2 Dispersion Shifted Fibers**

The other two profiles to be examined are fibers F3 and F4 shown in Figures 3.1b and 3.1c, respectively. The two fibers are characterized by their depressed core, where the first cladding has the largest refractive index instead of the core. The materials of fibers F3 and F4 and their radii are summarized in Table 3.4.

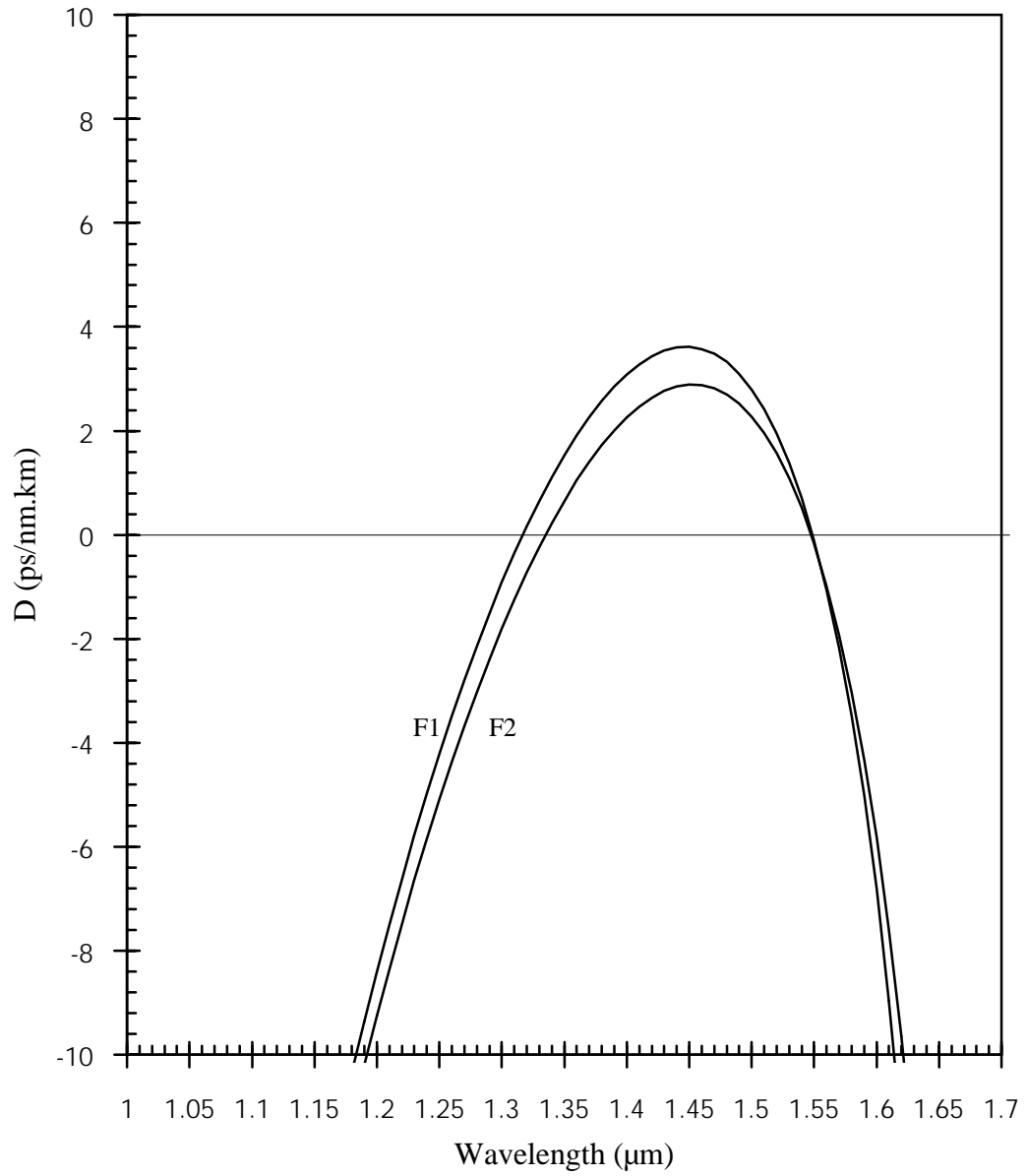


**Figure 3.5 Dispersion versus wavelength for the y-polarization of fundamental  $LP_{01}$  mode for fibers F1 and F2.**

**Table 3.4 Materials and Radii for Polarization-Maintaining Dispersion-Shifted and -Unshifted Fibers.**

Fiber	Index Profile	Core	Clad1	Clad2	Clad3
F3	Fig. 3.1b	M10 3.2 $\mu\text{m}$	M2 3.9 $\mu\text{m}$	M3 $\infty$	—
F4	Fig. 3.1c	M11 1.5 $\mu\text{m}$	M9 3 $\mu\text{m}$	M12 5.1 $\mu\text{m}$	$\infty$
F5	Fig. 3.1d	M14 3.5 $\mu\text{m}$	M6 3.8 $\mu\text{m}$	M7 4.5 $\mu\text{m}$	M4 $\infty$

Variations of propagation constant  $b$  for the  $y$  and  $x$  polarizations of the fundamental  $LP_{01}$  mode, versus wavelength are displayed in Figures 3.2 and 3.3, respectively. For fiber F4, the propagation constant of the  $x$ -polarized fundamental mode has a higher value than that of fiber F3 over the wavelength range  $1 \mu\text{m} < \lambda < 1.22 \mu\text{m}$ , and the same holds true for the  $y$ -polarization except that the wavelength range here is  $1 \mu\text{m} < \lambda \leq 1.47 \mu\text{m}$ . Beyond the upper wavelength range stated, the propagation constant  $b$  of both polarizations  $x$  and  $y$  for fiber F3 becomes higher than that of F4. The cutoff wavelength for the  $y$ -polarized fundamental mode in both fibers is the same,  $\lambda = 1.89 \mu\text{m}$ , while they are different for the  $x$ -polarization modes. The cutoff wavelength for the  $x$ -polarized fundamental mode is about  $\lambda = 1.89 \mu\text{m}$  and  $1.79 \mu\text{m}$  for fibers F3 and F4, respectively. Table 3.3 shows that the cutoff wavelength for the next higher  $y$ -polarized mode is less than  $1.15 \mu\text{m}$  for fiber F3, and less than  $0.96 \mu\text{m}$  for fiber F4. Therefore, the only modes that exist in the wavelength range  $1.15 \mu\text{m} < \lambda < 1.89 \mu\text{m}$  are the  $x$ - and  $y$ -polarized fundamental modes. Examining the birefringence versus wavelength shown in Figure 3.4, it is clear that fiber F4 has a higher birefringence than fiber F3 over the wavelength range  $1 \mu\text{m} < \lambda < 1.7 \mu\text{m}$ , and then its birefringence becomes lower than that of fiber F3 beyond  $\lambda = 1.7 \mu\text{m}$ . The birefringence of fibers F3 and F4 becomes equal to about  $1.3 \times 10^{-4}$  at  $\lambda = 1.69 \mu\text{m}$ . At  $\lambda = 1.55 \mu\text{m}$  the birefringence is found to be  $1.48 \times 10^{-4}$  and  $2.2 \times 10^{-4}$  for fibers F3 and F4, respectively.

The dispersion of the y-polarized fundamental mode at  $\lambda = 1.55 \mu\text{m}$  for fibers F3 and F4 is 0.0364 ps/nm.km and 0.082 ps/nm.km, respectively. Also, from the dispersion versus wavelength graph for the y-polarized fundamental mode shown in Figure 3.6, the dispersion slope for fiber F4 is larger than the slope of fiber F3, and therefore there is less variation in dispersion value when operating below or above 1.55  $\mu\text{m}$  for fiber F3 than fiber F4.

### 3.3.1.3 Dispersion-Unshifted Fibers

In an alternative design, the goal is to achieve a high birefringence and zero dispersion at a wavelength in the 1.3  $\mu\text{m}$  window, say at 1.33  $\mu\text{m}$ . In general, the main application in operating at this wavelength is found in sensing devices, such as gyroscopes, that require a polarized output at the end of the fiber, but 1.3  $\mu\text{m}$  polarization-preserving fibers are also of interest in communication systems. The fiber profile chosen to be examined for such purpose is that shown in Figure 3.1d and its material compositions and radii are summarized in Table 3.4 as F5. Previous discussions of birefringence properties indicated that higher birefringence is obtained at wavelengths lower than 1.55  $\mu\text{m}$ . This feature can be seen for the profile at hand in Figure 3.4, where the birefringence at 1.33  $\mu\text{m}$  wavelength is higher than those at higher wavelengths. From Figure 3.4, the birefringence at 1.33  $\mu\text{m}$  is estimated to be about  $4.9 \times 10^{-4}$ . Also, nearly zero dispersion is achieved at 1.33  $\mu\text{m}$  wavelength ( $D = 0.056 \text{ ps/nm.km}$ ) as shown in Figure 3.6, and small variations of dispersion value around the region of 1.33  $\mu\text{m}$  wavelength. Both the x- and y-polarizations have cutoff wavelength higher than 1.7  $\mu\text{m}$ , as illustrated in Figures 3.2 and 3.3. Some of the previous profiles discussed previously can be optimized to operate at lower wavelengths too.



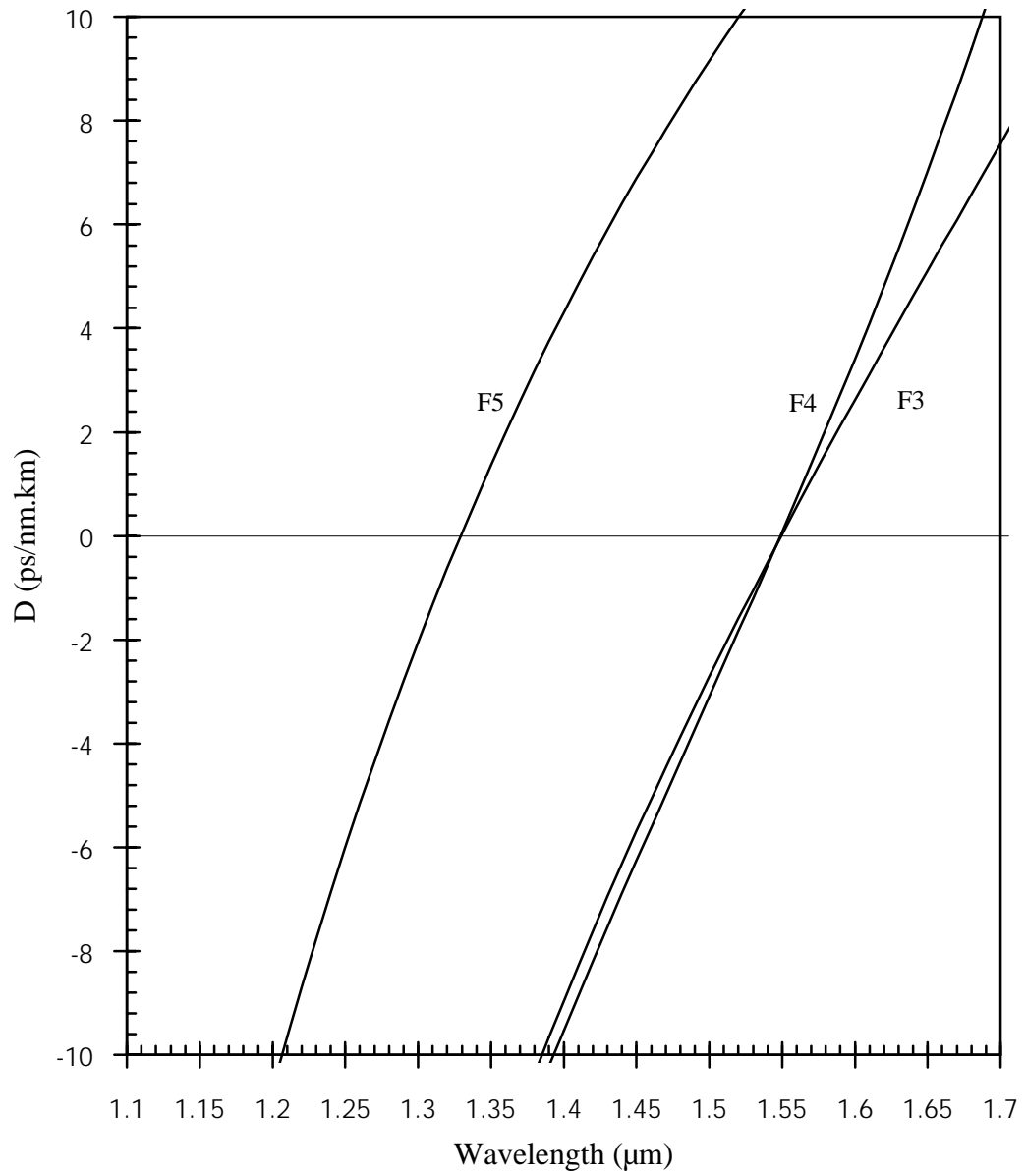


**Figure 3.6 Dispersion versus wavelength for the y-polarization of fundamental  $LP_{01}$  mode for fibers F3 to F5.**

### 3.3.2 Single-Polarization Single-Mode Fibers (SPSM)

So far, we have discussed high-birefringence fibers that can maintain a single-polarization fundamental mode by reducing the coupling between the two polarizations of the fundamental modes. However, increasing the length of such fibers in coherent communication applications could cause crosstalk degradation. The ultimate remedy is the single-polarization single-mode fiber which is a truly single-mode fiber. The principle of operation for SPSM fibers is that they propagate one and only one polarization state of the fundamental mode.

Single-polarization single-mode fibers have been studied and investigated before. Two techniques have been used to make these fibers. In the first technique, the fiber is designed such that one polarization of the fundamental modes is unguided. The second method is based on maintaining a large differential loss between the two polarizations of the fundamental mode [67].

In this study, the first technique is adopted to achieve single-polarization single-mode fiber designs. The goal is to achieve single-mode and single-polarization operation as well as zero dispersion at  $\lambda = 1.33 \mu\text{m}$  and/or  $1.55 \mu\text{m}$ .

#### 3.3.2.1 Single-Polarization Single-Mode Dispersion-Flattened Fibers

Some of the profiles introduced in the previous sections as well as some additional ones will be used to design SPSM fibers. The principal design criterion is to have the cutoff of one polarization of the fundamental mode above and the cutoff of the other polarization below the wavelength of operation. The cutoff of either polarization occurs when its propagation constant  $\bar{\beta}$  becomes equal to the refractive index of the outer cladding layer; that is,  $\bar{\beta}_x$  or  $\bar{\beta}_y = n_{cl}$  of outer layer. Equivalently, for a certain polarization to be cutoff, the following condition must be met, [67] and [112],

$$\int_A (n_j^2 - n_{cl}^2) dA < 0 \quad (3.9)$$

where  $n_j$  is the refractive-index of either x- or y-polarization,  $n_{cl}$  is the refractive index of the outer cladding layer, and  $A$  is the area of the waveguide cross section.

The material compositions and the dimensions of fibers designed as SPSM are chosen and optimized so that the x-polarization of the fundamental mode is cutoff, while the y-polarization remains guided. Moreover, low or zero dispersion at 1.33  $\mu\text{m}$  and 1.55  $\mu\text{m}$  is of primary concern in this study, therefore the optimum design presented here will meet three requirements: single polarization, single-mode operation, and low dispersion.

The design process is initiated with the W-type profile shown in Figure 3.1a, for which the material composition and layers' radii are summarized in Table 3.5 as fiber F6.

Figure 3.7 shows variations of the normalized propagation constant  $b$  versus wavelength. The width of the single-polarization region, in which only the y-polarization mode exists as a guided mode is determined to be about 100 nm and centered at 1.55  $\mu\text{m}$ . Also, the low dispersion at 1.33  $\mu\text{m}$  and 1.55  $\mu\text{m}$  has been achieved as can be seen in Figure 3.8. The dispersion is found to be about -0.75 ps/nm.km and 0.91 ps/nm.km at 1.33  $\mu\text{m}$  and 1.55  $\mu\text{m}$ , respectively. The dispersion variation versus wavelength in Figure 3.8 shows that the dispersion has less variation around the 1.33  $\mu\text{m}$  wavelength region than around the 1.55  $\mu\text{m}$  wavelength region.

Next, an examination of a different index profile and optimization of design will be carried out to achieve a single-polarization and single-mode operation with zero dispersion at 1.55  $\mu\text{m}$ . The profile chosen is a triple-clad fiber and is shown in Figure 3.1d. The material compositions and radii are summarized in Table 3.5 as F7. The same profile shape was considered previously for fiber F2, as a high-birefringence fiber. The composition of layers' material are chosen to be the same for the present application. The profile also can be used to design a single-polarization single-mode fiber. It provides, as seen from Figure 3.7, a single-polarization operation at 1.55  $\mu\text{m}$  with a single-mode operation width of 100 nm. This profile also provides almost zero dispersion (0.096 ps/nm.km

**Table 3.5 Materials and Radii of Designed SPSM Fibers.**

Fiber	Index Profile	Core	Clad1	Clad2	Clad3
F6	Fig. 3.1a	M10 3.4 $\mu\text{m}$	M1 7 $\mu\text{m}$	M8 $\infty$	—
F7	Fig. 3.1d	M14 2.8 $\mu\text{m}$	M12 3.2 $\mu\text{m}$	M13 7.5 $\mu\text{m}$	M4 $\infty$
F8	Fig. 3.1e	M10 1.75 $\mu\text{m}$	M1 3.8 $\mu\text{m}$	M8 5 $\mu\text{m}$	M13 $\infty$
F9	Fig. 3.1e	M10 1 $\mu\text{m}$	M1 3.6 $\mu\text{m}$	M8 6 $\mu\text{m}$	M13 $\infty$

and 0.038 ps/nm.km) at two wavelengths 1.33  $\mu\text{m}$  and 1.55  $\mu\text{m}$ , respectively. As shown in Figure 3.8, this type of fiber is a dispersion flattened as was fiber F6, however, F7 provides lower dispersion in the 1.33  $\mu\text{m} < \lambda < 1.55 \mu\text{m}$  range than fiber F6. Examination of the dispersion curves of fibers F6 and F7 shown in Figure 3.8, indicates that both fibers have the same dispersion slope around the 1.55  $\mu\text{m}$  range, but F7 has smaller dispersion slope around the 1.33  $\mu\text{m}$  wavelength range than F6.

### 3.3.2.2 Single-Polarization Single-Mode Dispersion-Shifted Fibers

In order to achieve a wider single-mode region while keeping low or zero dispersion, a profile is formed by incorporating an additional cladding layer into the W-fiber used for F6. The result is a three-clad fiber shown in Figure 3.1e with material compositions and radii summarized in Table 3.5 as fiber F8. From Figure 3.9, displaying the variation of the normalized propagation constant versus wavelength for x- and y-polarization of the fundamental mode, the width of single-polarization single-mode operation is determined to be at least 200 nm for operation in the 1.55  $\mu\text{m}$  window. The dispersion characteristic for fiber F8 is illustrated in Figure 3.10. It is noted that dispersion is about zero at 1.55  $\mu\text{m}$  and there is much smaller dispersion slope compared to the former profile F6. Fiber F6 is

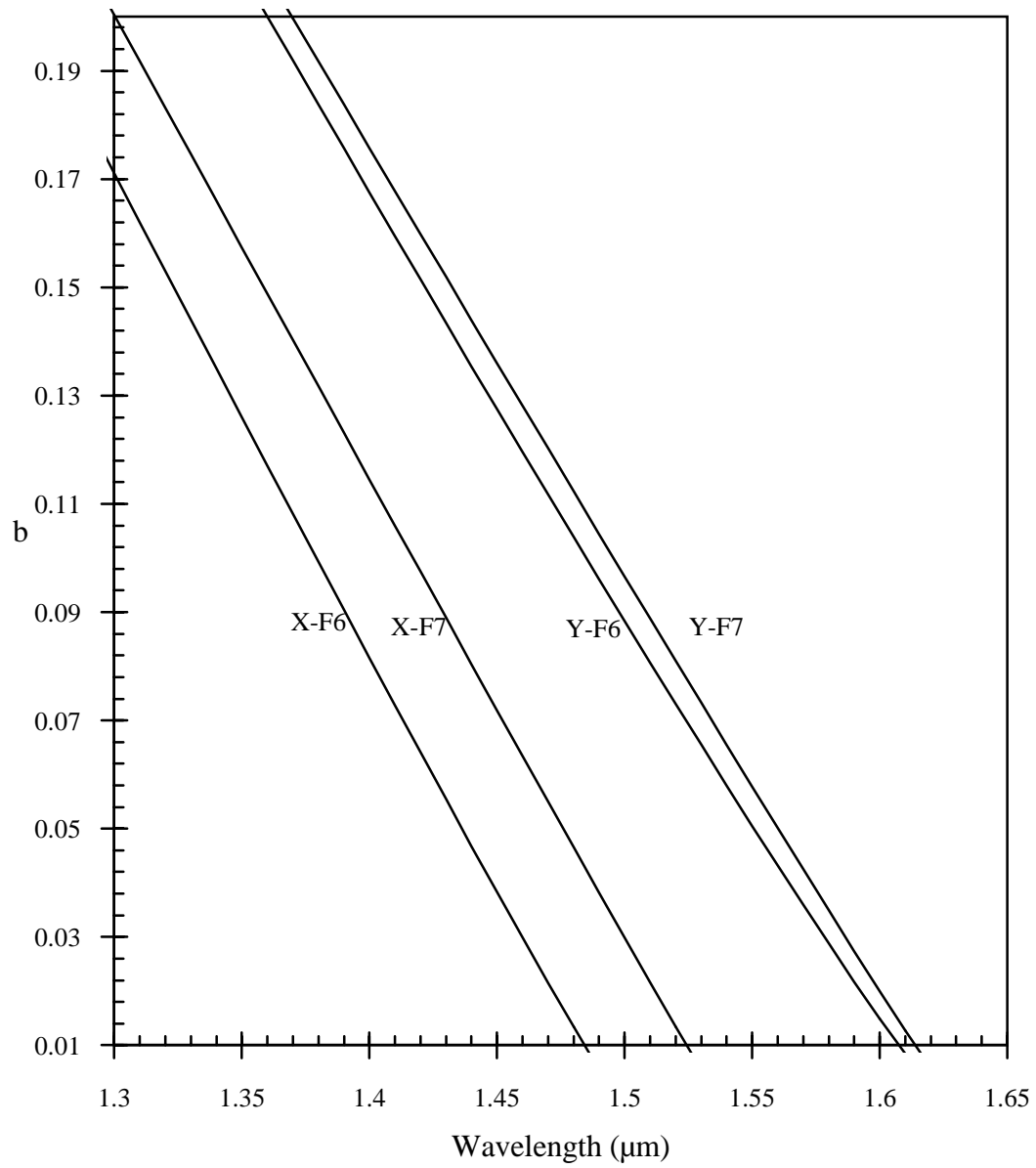


**Figure 3.7 Normalized propagation constant versus wavelength for the x and y polarizations of fundamental LP<sub>01</sub> mode for fibers F6 and F7.**

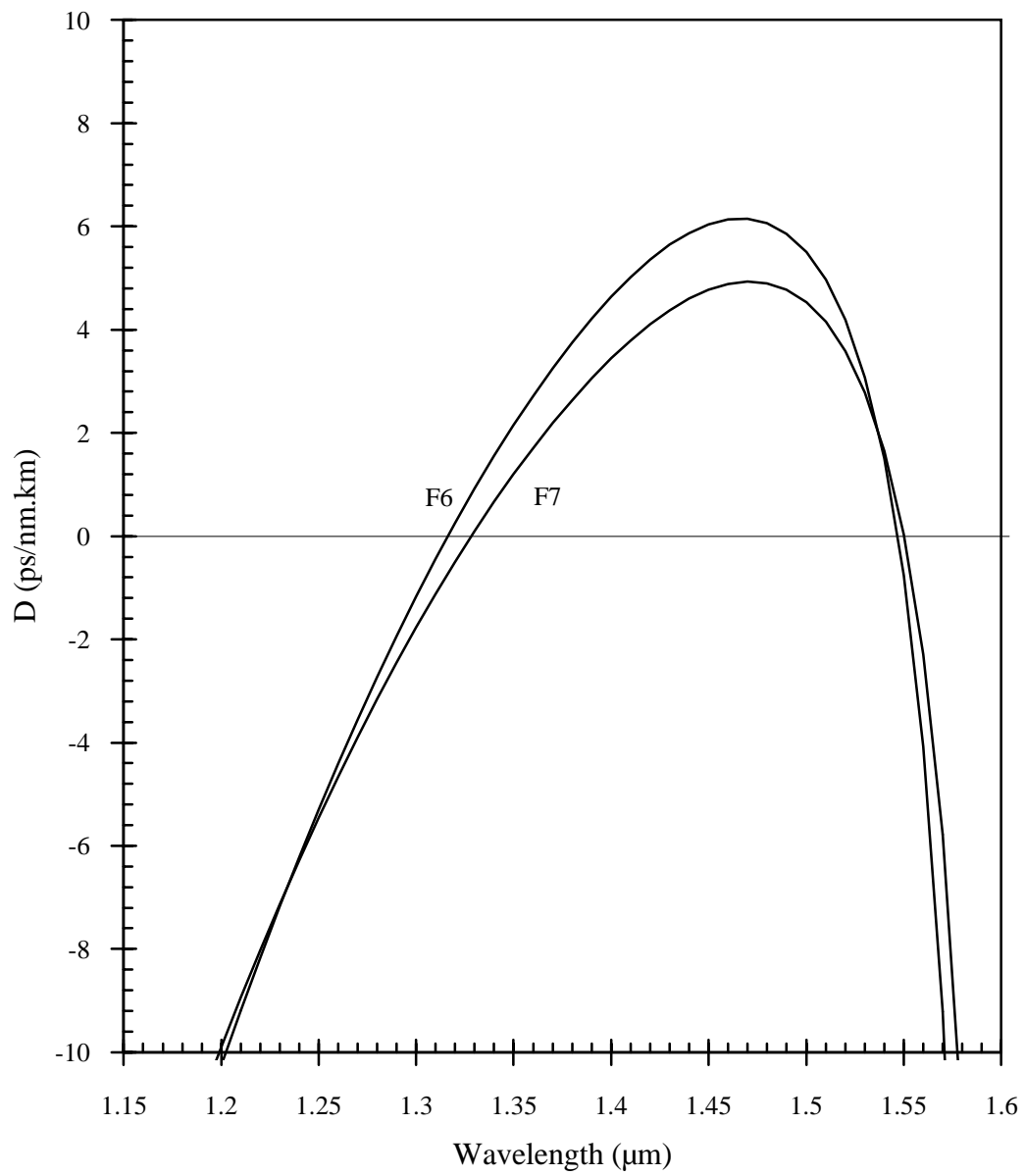


**Figure 3.8 Dispersion versus wavelength for the y-polarization of fundamental  $\text{LP}_{01}$  mode for fibers F6 and F7.**

a dispersion flattened fiber which provides low dispersion at two wavelengths 1.33  $\mu\text{m}$  and 1.55  $\mu\text{m}$ .

### **3.3.2.3 Single-Polarization Single-Mode Dispersion-Unshifted Fibers**

In previous fiber designs, the attempt was to obtain a single-polarization single-mode fiber with zero dispersion for operation at 1.55  $\mu\text{m}$ . Now, the attempt is to obtain a single-polarization single-mode fiber with zero dispersion operating at a wavelength of about 1.3  $\mu\text{m}$ . The profile considered is that shown in Figure 3.1e. This profile was considered previously for fiber F8, but with different dimensions than those considered here for fiber F9. In order for this fiber to operate as a single-polarization mode, the necessary material compositions and optimized radii are summarized in Table 3.5 as fiber F9. In order for this fiber to operate as a single-polarization single-mode fiber, the necessary material compositions and radii are summarized in Table 3.5. The normalized propagation constant and the dispersion versus wavelength are shown in Figures 3.9 and 3.10, respectively. As seen in Figure 3.9, a single-polarization wavelength range is achieved for  $\lambda > 1.15 \mu\text{m}$ . The total single-polarization wavelength width is more than 500 nm, and the y-polarized mode can be operated freely at 1.33  $\mu\text{m}$  or anywhere in this wavelength window 1.33  $\mu\text{m}$ . The estimated value of dispersion at  $\lambda = 1.33 \mu\text{m}$  is 1.73 ps/nm.km.

Characteristics of the polarization-maintaining fibers discussed in this Chapter are summarized in Table 3.6.

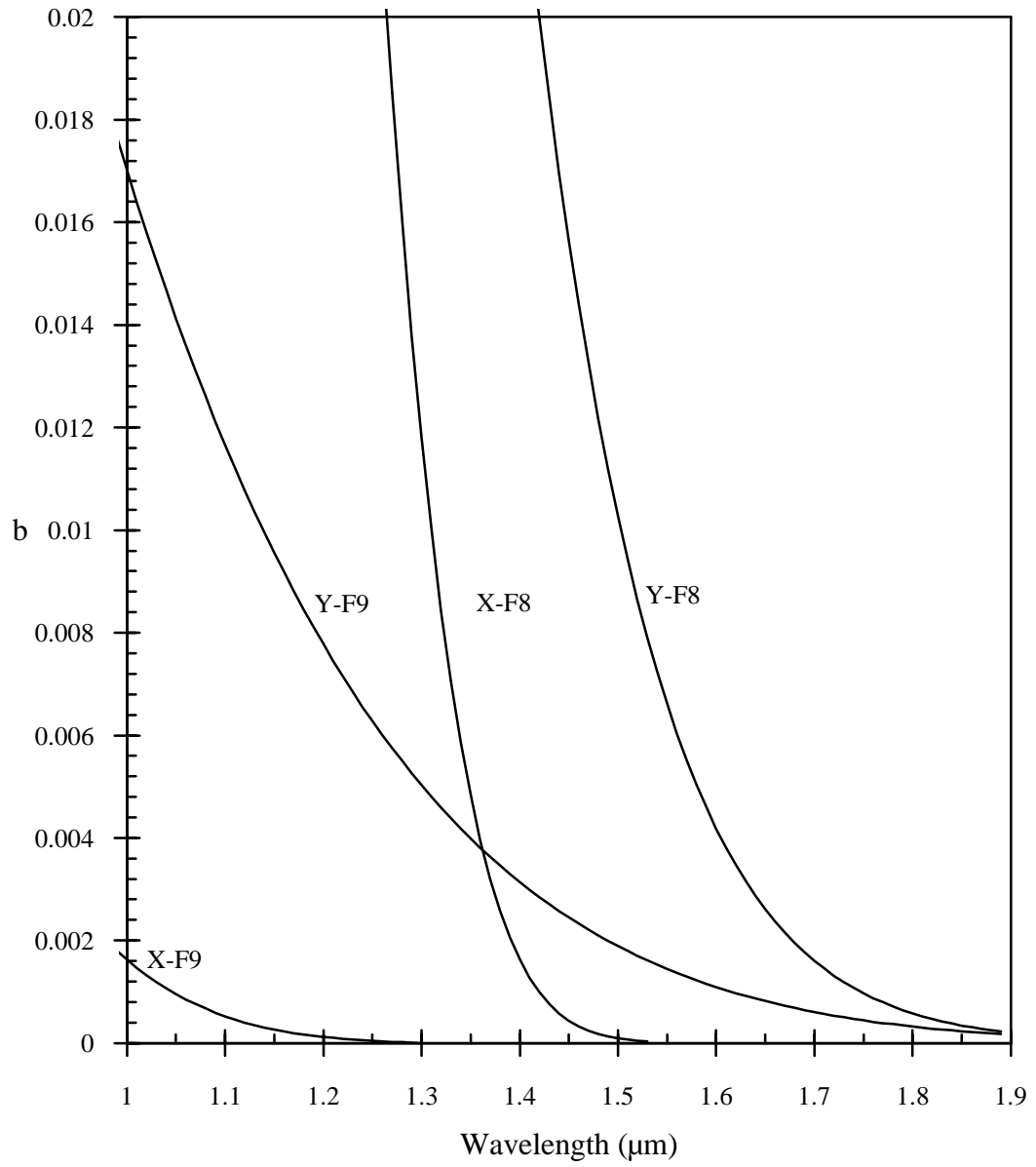


**Figure 3.9** Normalized propagation constant versus wavelength for the x and y polarizations of fundamental  $\text{LP}_{01}$  mode for fibers F8 and F9.



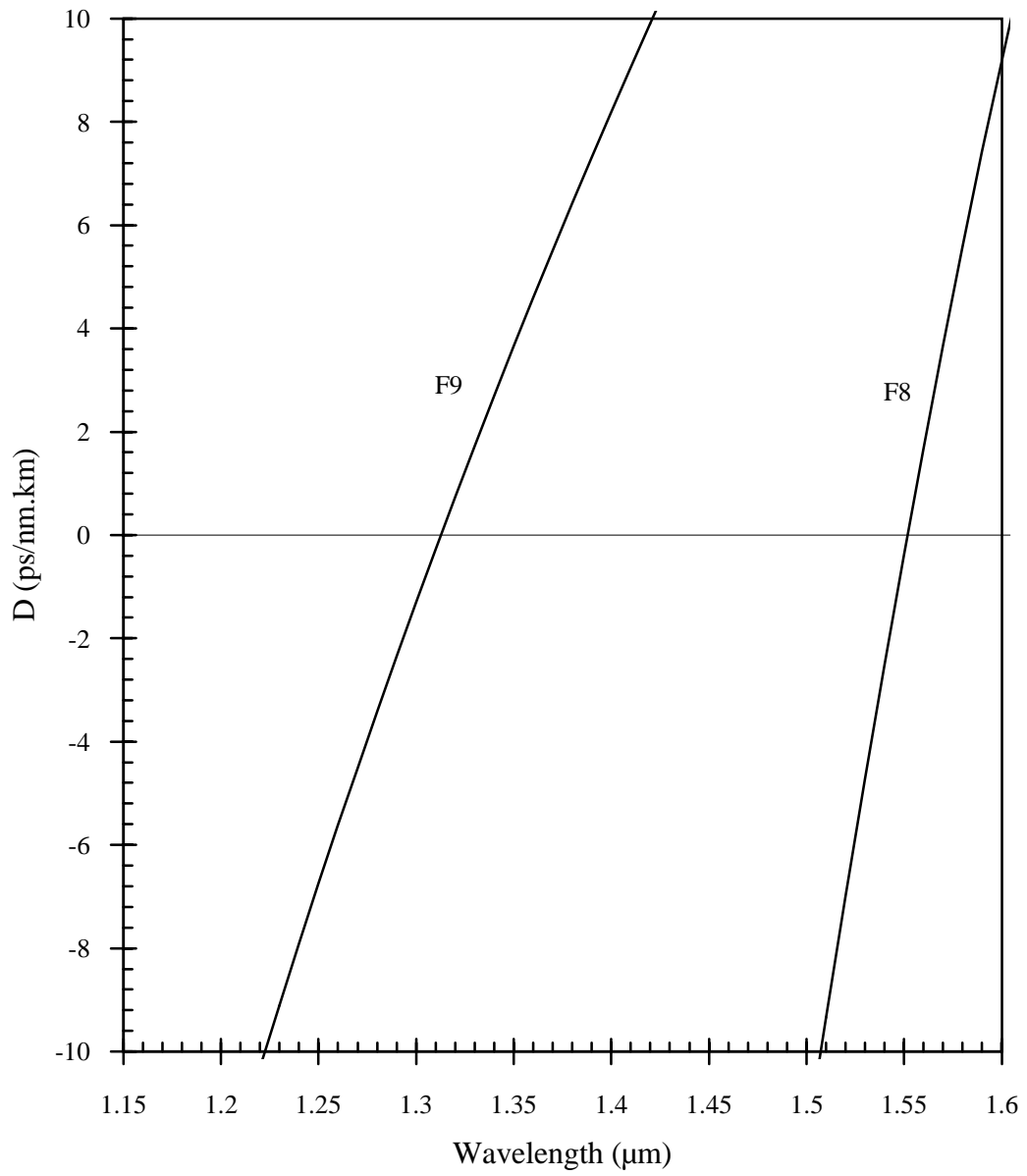


**Figure 3.10 Dispersion versus wavelength for the y-polarization of fundamental  $\text{LP}_{01}$  mode for fibers F8 and F9.**

**Table 3.6 Summary of Characteristics For The Designed Polarization-Maintaining Fibers.**

Fiber	Birefringence at		Dispersion (ps/nm.km) at		Wavelength ( $\mu\text{m}$ ) of Zero Dispersion	SPSM Wavelength Range ( $\mu\text{m}$ ) For LP <sub>01</sub> Mode
	1.33 $\mu\text{m}$	1.55 $\mu\text{m}$	1.33 $\mu\text{m}$	1.55 $\mu\text{m}$		
<b>F1</b>	$5.11 \times 10^{-4}$	$4.87 \times 10^{-4}$	0.65	-0.1	1.315 & 1.545	–
<b>F2</b>	$5.11 \times 10^{-4}$	$4.87 \times 10^{-4}$	-0.23	-0.16	1.335 & 1.545	–
<b>F3</b>	–	$1.48 \times 10^{-4}$	–	0.0364	–	–
<b>F4</b>	–	$2.2 \times 10^{-4}$	–	0.082	–	–
<b>F5</b>	$4.9 \times 10^{-4}$	–	0.056	–	–	–
<b>F6</b>	–	–	–	-0.75	1.545	1.49-1.62
<b>F7</b>	–	–	–	0.038	–	1.53-1.62
<b>F8</b>	–	–	–	-0.39	1.555	1.41-1.75
<b>F9</b>	–	–	1.729	–	1.315	1.15-1.63